

Supporting Information

Water-Mediated Charge Transfer and Electron Localization in a Co_3Fe_2 Cyanide-Bridged Trigonal Bipyramidal Complex

Emily Hruska¹, Quansong Zhu¹, Somnath Biswas¹, Matthew T. Fortunato¹,
Dustin R. Broderick¹, Christine M. Morales², John M. Herbert¹, Claudia Turro¹,
and L. Robert Baker^{1*}

¹*Department of Chemistry and Biochemistry, The Ohio State University, Columbus, OH
43210*

²*Department of Chemistry, University of Mount Union, Alliance, OH 44601*

E-mail: baker.2364@osu.edu

Contents

1. Sample Preparation
 - A. Materials
 - B. $[\text{Co}(\text{tmphen})_2]_3[\text{Fe}(\text{CN})_6]_2$ (Co_3Fe_2)
 - C. Co_3Fe_2 characterization
 - D. Co_3Fe_2 solution
 - E. Solution drop-casting
2. XPS Fitting Parameters

3. NAP-XPS Controls
 - A. Conditional exposure
 - B. X-ray exposure
 - C. Solvent photoionization
 - D. CO exposure
 - E. N $1s$ solvent exposure
 - F. C $1s$ solvent exposure
4. SFG Controls
 - A. Clean substrate baseline
 - B. Time delay interference
 - C. Sample pseudo-homogeneity
5. Single-Crystal X-ray Structure
6. DFT-Optimized Structures
 - A. $S = 3/2$ state
 - B. $S = 9/2$ state

1. Sample Preparation

A. Materials

Acetonitrile, methanol, and 3,4,7,8-tetramethyl-1,10-phenanthroline (tmphen) were purchased from Fisher Scientific; the solvents were distilled prior to use. Potassium hexacyanocobaltate(III), potassium ferricyanide, and 18-crown-6 were procured from Sigma-Aldrich. Cobalt nitrate $\text{Co}(\text{NO}_3)_2 \cdot 6\text{H}_2\text{O}$ was obtained from Baker & Adamson, and ferrocenium tetrafluoroborate was purchased from Alfa. Mineral oil, suitable for preparation of Nujol mulls for infrared spectroscopy was purchased from Sigma-Aldrich. Solvents and reagents were used as received unless otherwise stated.

B. $[\text{Co}(\text{tmphen})_2]_3[\text{Fe}(\text{CN})_6]_2$ (Co_3Fe_2)

18-crown-6 (406 mg, 1.54 mmol) was added to a solution of $\text{K}_3[\text{Fe}(\text{CN})_6]$ (178 mg, 0.541 mmol) in 60 mL of acetonitrile in air, and the mixture was stirred overnight to solubilize ferricyanide by caging the potassium ion within the cryptand to generate $[(18\text{-crown-6})]_3[\text{Fe}(\text{CN})_6]$. The solution was filtered to remove residual $\text{K}_3[\text{Fe}(\text{CN})_6]$. The $[(18\text{-crown-6})]_3[\text{Fe}(\text{CN})_6]$ solution was slowly added to a mixture of $\text{Co}(\text{NO}_3)_2 \cdot 6\text{H}_2\text{O}$ (305 mg, 1.04 mmol) and tmphen (601 mg, 2.54 mmol) and dissolved in 150 mL CH_3CN . The mixture was allowed to stand for 2 days which resulted in red crystals. A yield of 37% (205 mg, 0.100 mmol) was achieved.

C. Co_3Fe_2 characterization

Three distinct IR bands are observed in Co_3Fe_2 at 2060 cm^{-1} , 2104 cm^{-1} , and 2133 cm^{-1} in Figure S1. The lower energy band at 2060 cm^{-1} was previously assigned to the terminal cyanide stretch, $\nu(\text{CN})_{\text{terminal}}$, and the two higher energy peaks correspond to the bridging ligands, $\nu(\text{CN})_{\text{bridging}}$, where the stretch at 2104 cm^{-1} was assigned to $\text{Fe}^{2+} - \text{CN} - \text{Co}^{3+}$ and that at 2133 cm^{-1} to $\text{Fe}^{2+} - \text{CN} - \text{Co}^{2+}$.¹ For comparison, the $\nu(\text{CN})_{\text{terminal}}$ bands in

$\text{K}_3[\text{FeIII}(\text{CN})_6]$ and $\text{K}_4[\text{FeII}(\text{CN})_6]$ are observed at 2117 cm^{-1} and 2050 cm^{-1} , respectively, in Nujol,² and the position of the $\nu(\text{CN})$ stretches in these complexes have been shown to shift to higher energies when the CN^- ligand bridges two metal centers.³ These shifts are consistent with the assignments of $\nu(\text{CN})_{\text{terminal}}$ and $\nu(\text{CN})_{\text{bridging}}$ in Co_3Fe_2 . The ESI mass spectrum recorded for Co_3Fe_2 exhibits a parent ion peak at $m/z = 677$ that corresponds to $[\text{Co}(\text{tmphen})_2]_3[\text{Fe}(\text{CN})_6]_2 \cdot 3\text{H}_3^+$ with $z = 3+$.

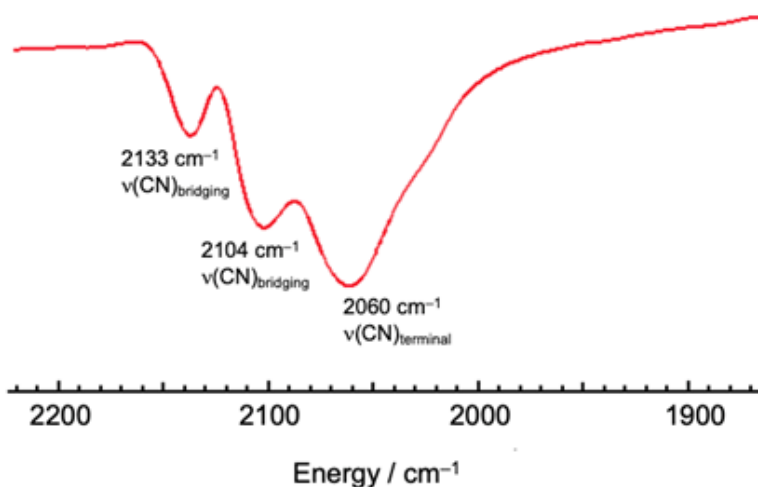


Figure S1: $\nu(\text{CN})$ region of the IR spectrum of Co_3Fe_2 in Nujol.

D. Co_3Fe_2 solution

For further spectroscopic studies included in the main manuscript, the synthesized blue powder sample was dissolved in various solvents to a deeply-colored saturation point, depending on the experimental requirements. In water, 6 mg of Co_3Fe_2 was dissolved for every 7 mL water. In methanol, 6 mg of Co_3Fe_2 was dissolved for every 2 mL methanol. In acetonitrile, 0.72 g of Co_3Fe_2 was dissolved for every 9 mL of acetonitrile. In glycerol, 2 mg of Co_3Fe_2 was dissolved in 0.5 mL of 60 wt.% glycerol solution. In all cases, the Co_3Fe_2 complex and solvent were mixed vigorously and left to stand for 24 hours to ensure dissolution.

E. Solution drop-casting

The NAP-XPS and Kratos XPS experiments took place on a substrate of 50 nm Ti on Au. The SFG experiments took place on a pure Au substrate. In both cases, the substrates were cleaned with a UV-ozone pre-treatment for 30 minutes followed by surface hydroxylation. The prepared Co_3Fe_2 solution was drop-cast on the surface of the clean Au substrate multiple times to build a uniform, concentrated layer. For the NAP-XPS and XPS measurements, 50 μL of the solution was dropped onto the surface 5 times per sample, allowing time for each layer to dry before re-saturating the surface. For the SFG experiments, 10 μL of the solution was dropped onto the surface 1 time per sample.

2. XPS Fitting Parameters

Because the temperature and pressure-dependent NAP-XPS spectra shown in the main manuscript represent a large sampling rate of individual spectra, significant standardization of the XPS fitting parameters was necessary. Specifically, each XPS spectrum is collected as a series of Co $2p$, Fe $2p$, O $1s$, N $1s$, and C $1s$ scans (in that order) cyclically collected 4 times per condition per sample. The purpose of this experimental order, rather than integrating at each core level for a longer time before proceeding to the next core level, was to eliminate the possibility for sample damage in unbalanced magnitudes as the binding energy shifted. The data resolution and spectral smoothness resulting was of high quality to use only one experiment per spectrum without need for significant data averaging.

The fitting parameters at the Fe and Co $2p$ core levels are represented in Table 1 (Fe) and Table 2 (Co) below. The constraints were modeled after previous reports for comparable metallic coordination motifs.⁴⁻⁹

Table S1: Fe $2p$ XPS fitting parameter constraints.

Component	Fe²⁺ 3/2 (A)	Fe³⁺ 3/2 (B)	Fe²⁺ 1/2	Fe³⁺ 1/2
Position	707.3	A + 1.3	A + 13.0	A + 15.0
FWHM	1.2 - 1.7	1.8 - 2.2	A * 1	B * 1
Area	–	–	A * 0.5	B * 0.5

Table S2: Co $2p$ XPS fitting parameter constraints.

Component	Co²⁺ 3/2 (A)	Co³⁺ 3/2 (B)	Co²⁺ 1/2 (C)	Co³⁺ 1/2
Position	779.9	A + 1.6	A + 15.6	A + 16.7
FWHM	1.6 - 2.0	A * 1	1.0 - 2.0	C * 1
Area	–	–	A * 0.5	B * 0.5

2. NAP-XPS Controls

While the NAP-XPS has been commissioned for both temperature and pressure-dependent photoemission experiments, several open questions arose while collecting measurements under steady gas flow. To address these other possible outcomes for the resulting spectra shown in the main manuscript, the following control experiments were performed.

A. Conditional exposure

One possibility for the spectroscopic change measured is a combination of X-ray exposure in the presence of gas phase solvent. To eliminate the possibility of exposure-dependent changes, two strategic experiments were performed.

Figure S2 shows a NAP-XPS measurement under UHV conditions of the Fe $2p$ core level on a Co_3Fe_2 sample prepared as described in section 1B above. First, a spectrum was collected at the same spot (Spot A) for 3 full cycles (4.5 hours of data collection). Then, the sample was shifted to a fresh spot (Spot B), which was not within the spot size of the X-ray source and therefore unexposed. Each of the Fe $2p$ core level spectra plotted with total CPS are within agreement. This indicates that the X-ray exposure under UHV conditions is not enough to induce a spectral change to the sample.

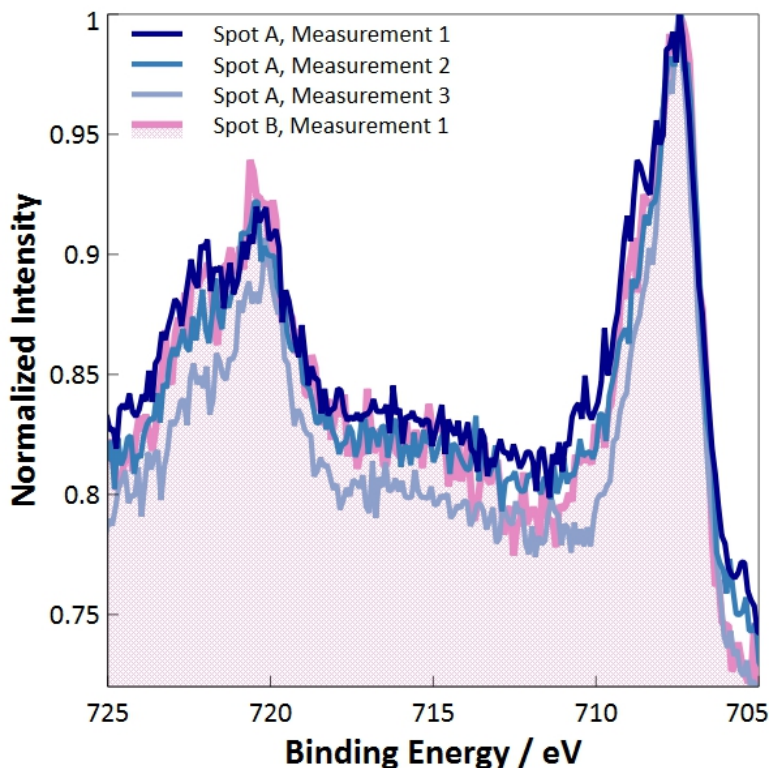


Figure S2: Fe $2p$ core level NAP-XPS measurements under UHV conditions. Spot A is measured three times in a row (blue x 3), and the final measurement is taken on a fresh spot B (pink).

Figure S3 shows a similar experiment with the introduction of water conditions. In this sequence, measurements proceeded on a fresh sample in the following order: (1) UHV on spot A, (2) 0.5 mbar water on spot A, (3) 2 mbar water on spot A, (4) 2 mbar water on spot B. On this sample, spot A experienced 3 hours of X-ray exposure and 1.5 hour of X-ray + water exposure before the final 2 mbar water spectrum plotted in dark red. Comparitively, spot B, plotted in orange, experienced no time of X-ray exposure before the plotted spectrum was collected. Again, the nearly identical lineshapes of the two results represent that the X-ray in combination with the presence of a solvent cannot account for a significant sample change, and the reversible dramatic spectral change seen in the Fe $2p$ core level is in fact due to a chemical state change.

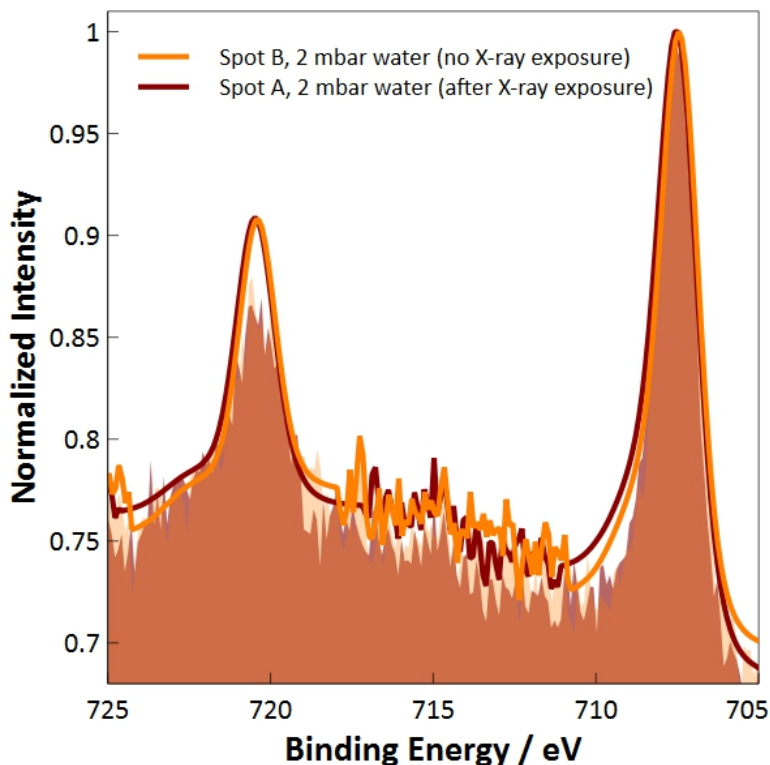


Figure S3: The NAP-XPS measurement was collected at 2 spots in the following order: UHV on spot A - 0.5 mbar on spot A - 2 mbar on spot A - 2 mbar on spot B. Spot A at 2 mbar water (red) and spot B at 2 mbar water (orange) overlay almost perfectly and show no apparent degradation in signal.

B. X-ray exposure

Another question presented with the NAP-XPS spectra is whether there could be persistent and progressive alterations to the sample state due to time-dependent X-ray exposure alone. To resolve this concern, multiple scans were collected in one condition and processed cyclically before stepping to a new condition and repeating the process. In this way, each spectrum would reveal whether there are steady changes due to beam exposure while maintaining a constant conditional pressure.

Figure S4 shows a contour plot of 12 experimental scans as a function of the normalized Fe $2p$ core level intensity. Scans 1-4 are UHV conditions, 5-8 are 0.5 mbar water, and 9-12 are 2 mbar water exposure. There are clear step edges from scans 4 to 5 and scans 8 to 9 around the $3/2$ and $1/2$ Fe features. Furthermore, there is no clear indication that the beam

exposure occurring between scans in the same condition had any effect on the spectra. These observations support the principle that the beam exposure had minimal effect on the samples and could not independently explain the large spectral differences visible as a function of solvent pressure.

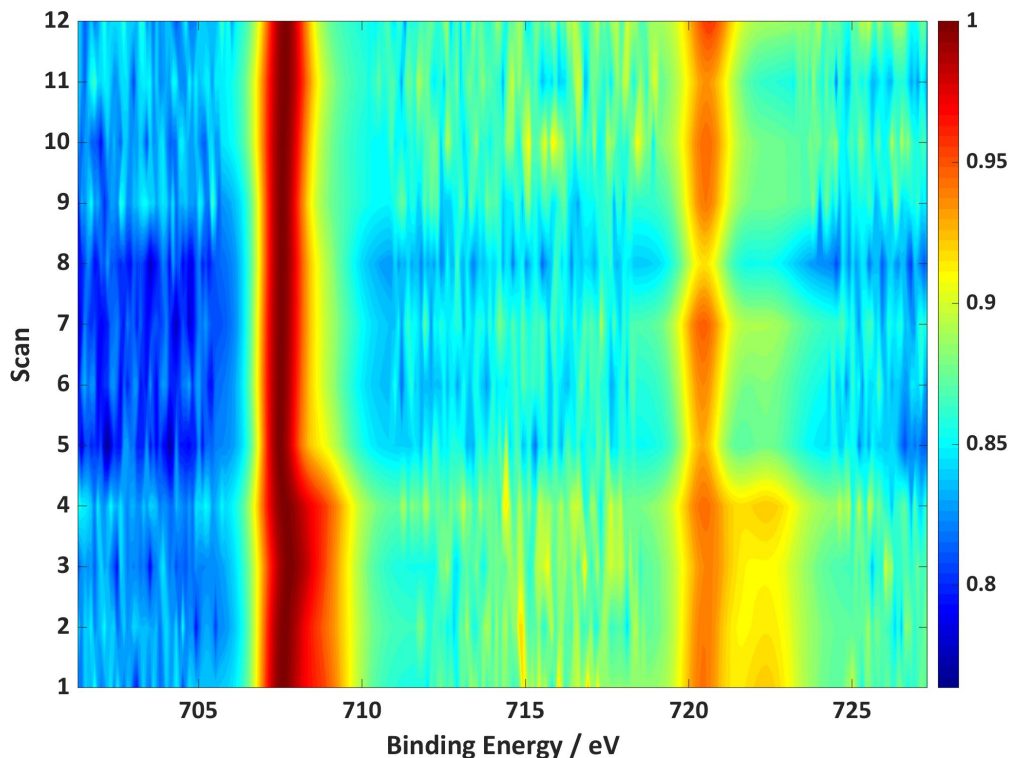


Figure S4: Countour plot of the binding energy (Fe $2p$ core level) versus scan number during an experiment, where scan 1-4 is UHV, scan 5-8 is 0.5 mbar water, and scan 9-12 is 2 mbar water. The intensity bar on the right side shows that the only significant intensity changes at the Fe features are between scans 4-5 and scans 8-9.

C. Solvent photoionization

A possible outcome of the presence of a gas phase solvent environment with the x-ray beam is photoionization of the solvent and subsequent electron attachment and reduction of the sample surface. We performed NAP-XPS measurements another solvent with a much higher photoionization cross section compared to water, carbon tetrachloride (CCl_4). Figure S5 below shows the results of this measurement, where a negligible change in either the Fe or

Co oxidation states as the sample is transitioned from UHV conditions to exposure to CCl_4 is seen. In fact, the Fe reduction between UHV and CCl_4 is 11.3%, compared to 83.4% in the case of water. This result supports the statement that X-ray ionization of the interacting solvent does not explain the reduction of Fe in the solvated environment.

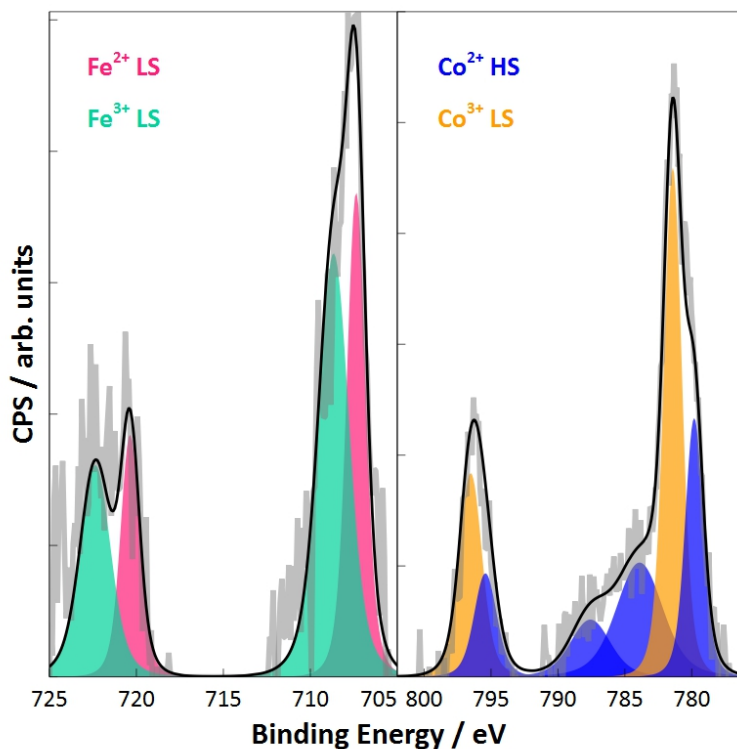


Figure S5: NAP-XPS results under exposure to CCl_4 . Total background-subtracted counts are shown as the gray solid line. The total fit is shown as the black solid line. Individual components are highlighted in pink (Fe^{2+}), green (Fe^{3+}), blue (Co^{2+}), and orange (Co^{3+}).

D. CO exposure

Figure S6 shows NAP-XPS results of the Fe and Co $2p$ regions cycling between UHV and 2 mbar CO exposure. This measurement, with no significant spectral change as a function of CO exposure, confirms that the change in peak shape in other gas environments is not the result of charging followed by sample neutralization in the presence of gas. Additionally, we can confirm here that there is no possibility of ligand exchange in these conditions.

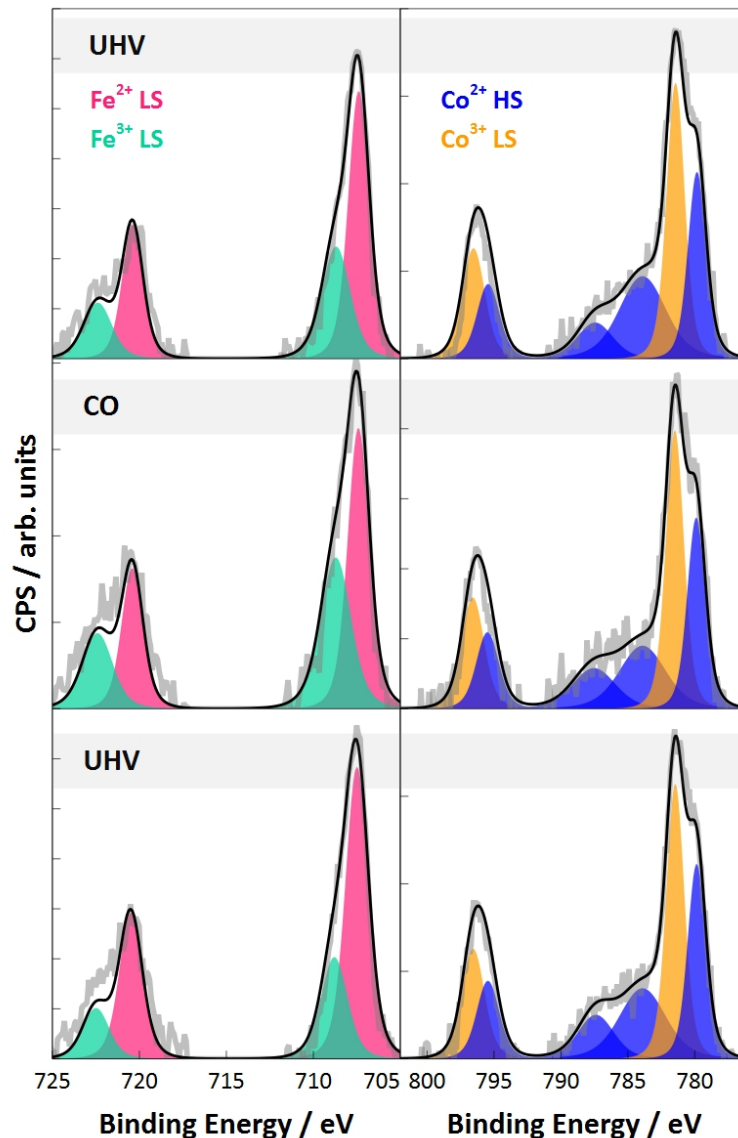


Figure S6: NAP-XPS results at UHV, CO, and post-exposure UHV of the Fe $2p$ (left) and Co $2p$ (right) core levels. Total background-subtracted counts are shown as the gray solid line. The total fit is shown as the black solid line. Individual components are highlighted in pink (Fe^{2+}), green (Fe^{3+}), blue (Co^{2+}), and orange (Co^{3+}).

E. N $1s$ solvent exposure

We evaluate the possibility of charge transfer between the metal sites and a phenanthroline ligand in Co_3Fe_2 . With NAP-XPS alone, this question is not directly addressed. Shown in Figure S7, the N $1s$ measurement does not show a significant spectral difference when

temperature and chemical environment are changed. Both of the two peaks, which can be assigned to the phenanthroline ligands (399 eV) and the cyanide ligands (397 eV), have steady position and intensity regardless of the environment. This suggests that the redox activity of the ligands in Co_3Fe_2 is not responsible for the reduction of the Fe shown in the main manuscript.

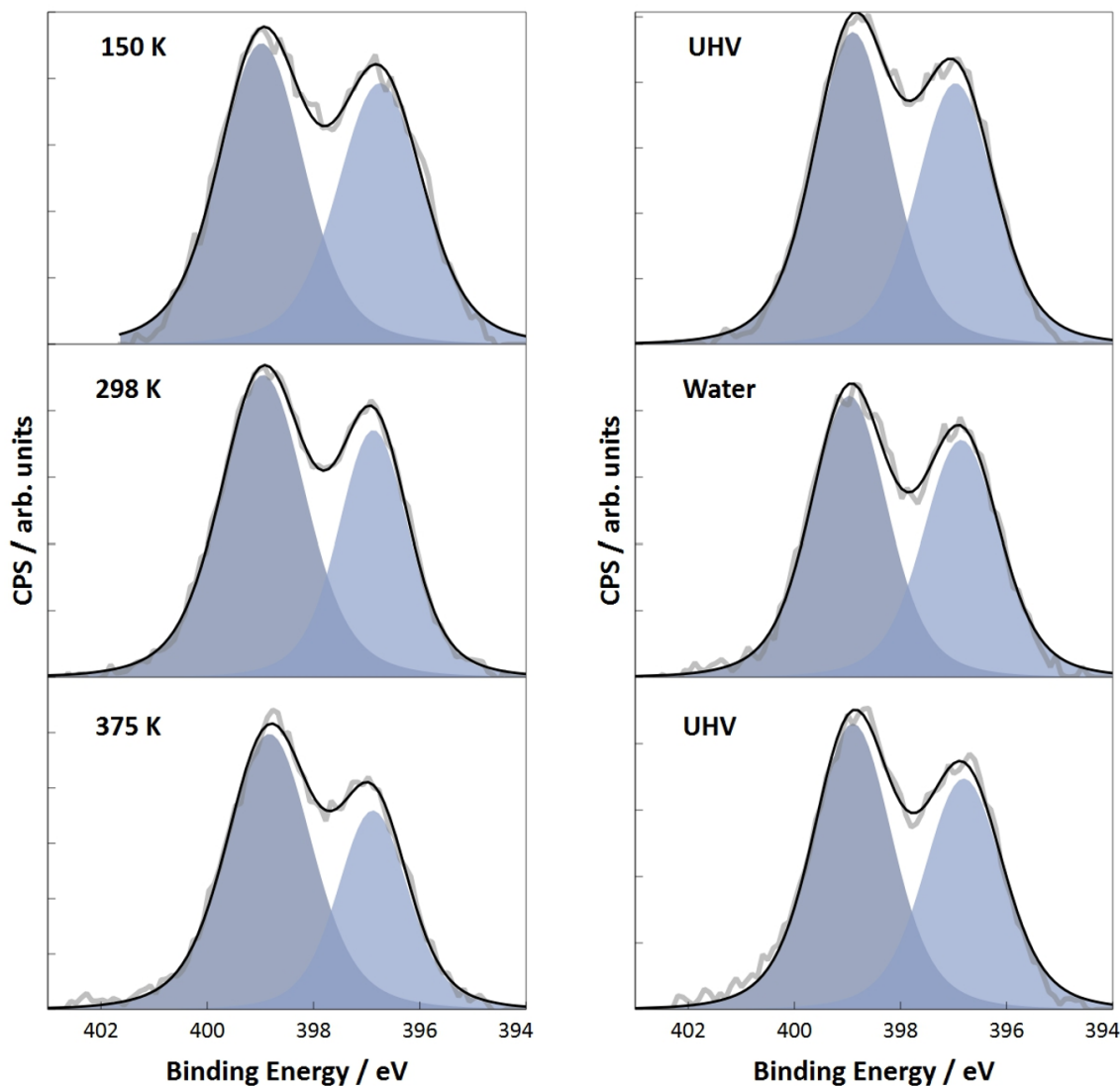


Figure S7: N $1s$ NAP-XPS measurement with cycling between (left) temperature from 150 - 375 K and (right) UHV, water, and UHV conditions. The gray line represents the raw CPS, the shaded regions are fits to the two peaks, and the black solid line is the envelope.

F. C $1s$ solvent exposure

We evaluate the C $1s$ region in Co_3Fe_2 to calibrate the NAP-XPS data and show the fits below to represent the validity of this calibration. Shown in Figure S8, the C $1s$ measurement does not show a significant spectral difference when chemical environment is changed. The central peak shifted to 284.5 eV has steady position and intensity regardless of the environment.

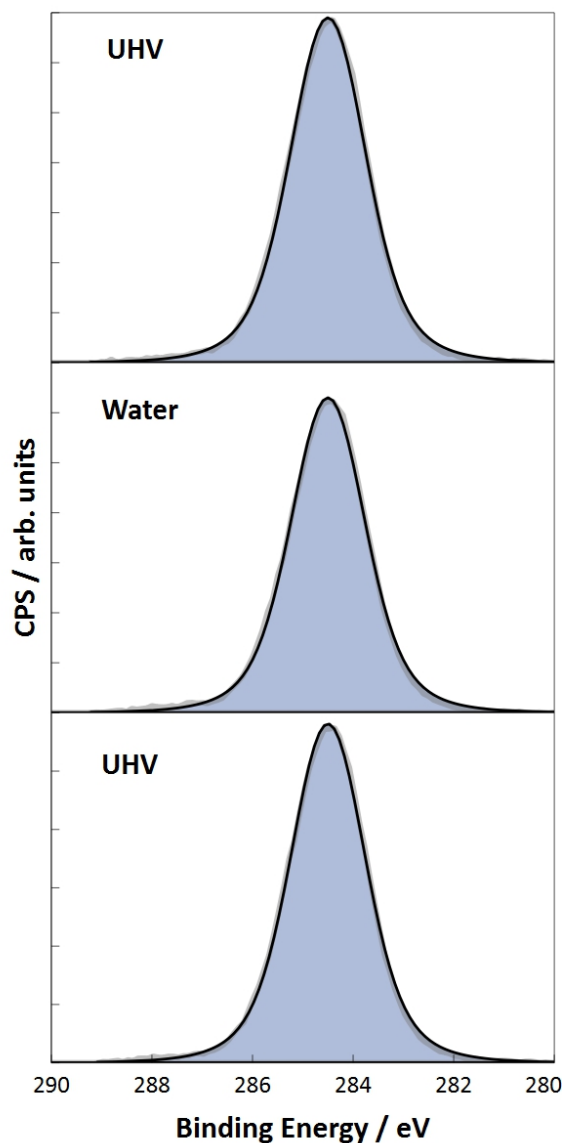


Figure S8: C $1s$ NAP-XPS measurement with cycling between UHV, water, and post-exposure UHV conditions. The gray line represents the raw CPS, the shaded regions are fits to the peaks, and the black solid line is the envelope.

4. SFG Controls

A. Clean substrate baseline

To confirm that the observed SFG signal is from Co_3Fe_2 without any contribution from the potential contamination on the Au substrate, SFG spectra were also taken for the ozone-treated bare Au sample under both Ar and water conditions, at the same acquisition condition as Co_3Fe_2 . As shown in Figure S9, SFG spectra for the bare Au substrate are very clean under both Ar and water purging conditions, showing no sign of contamination, which indicates the observed resonant features are solely from the Co_3Fe_2 complex.

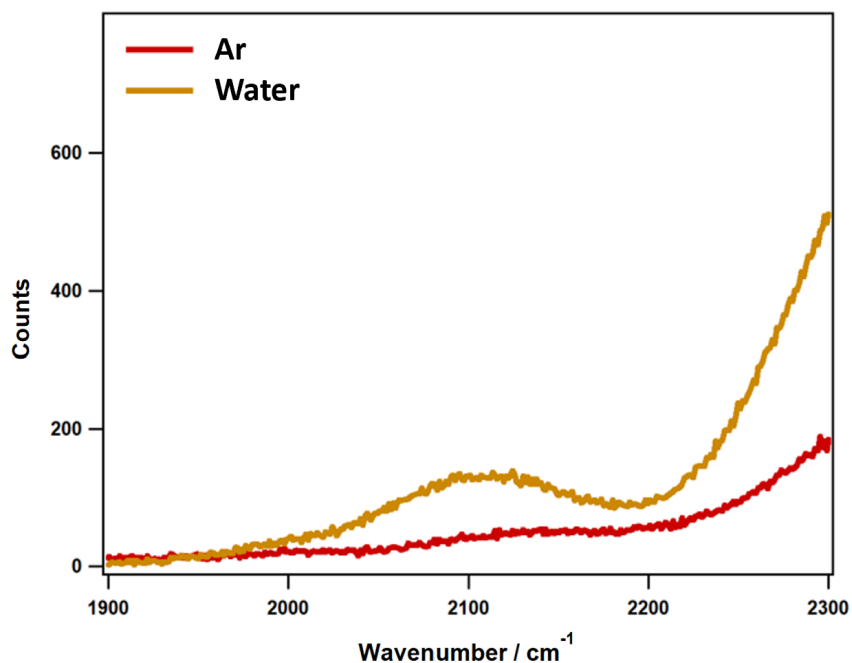


Figure S9: SFG spectra of the ozone-treated bare Au substrates under Ar and water purging conditions.

B. Time delay interference

To confirm that there is no significant contribution from non-resonant signal to the obtained SFG spectra, we took the non-resonant spectra on bare Au as a function of time delay under both Ar (Figure S10) and water (Figure S11) purging conditions. The non-resonant

signal is significantly suppressed as the time delay of the visible beam relative to the IR beam increases. It almost completely disappears at the delay of 670 fs. Under experimental conditions where the delay is about 850 fs, there should be no contribution from the non-resonant background to the SFG spectra.

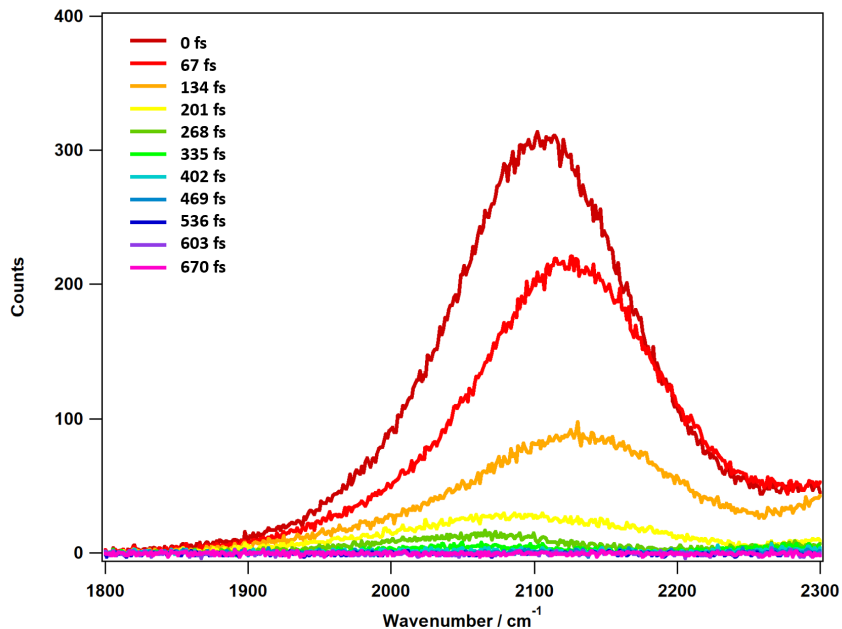


Figure S10: The non-resonant profile of bare Au as a function of time delay under Ar purging conditions.

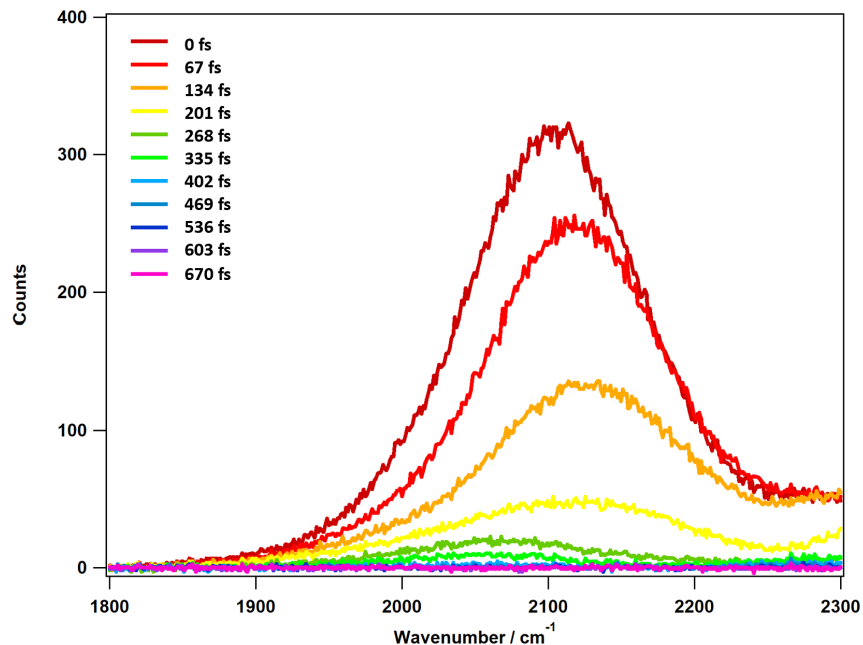


Figure S11: The non-resonant profile of bare Au as a function of time delay under water purging conditions.

C. Sample pseudo-homogeneity

To confirm that the obtained SFG features are consistent and uniform among the whole sample, we took SFG spectra at different spots on the drop-casted Co_3Fe_2 thin film. Figure S12 shows an example of the Ar purging case. Although the intensity varies from spot to spot, the major features are consistent, indicating a good homogeneity of the prepared sample and supporting that the observed features are real.

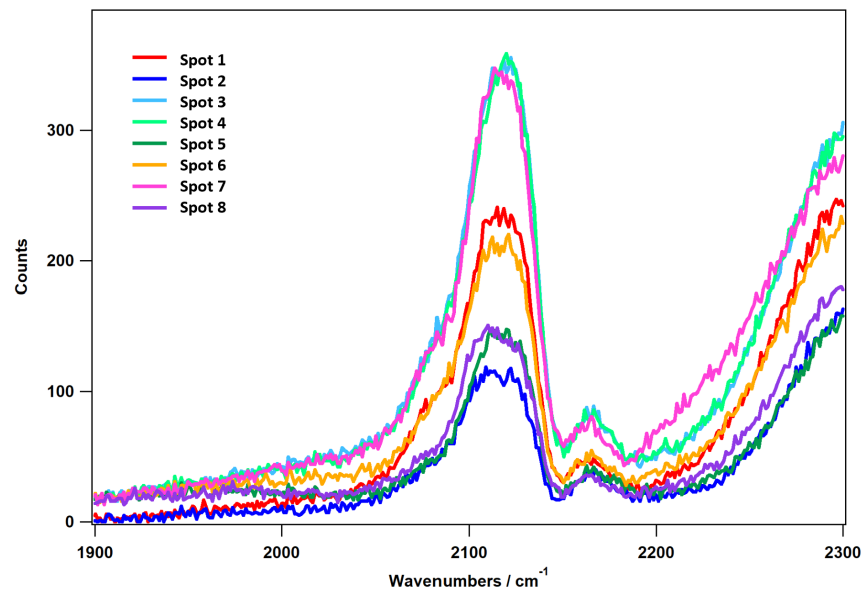


Figure S12: SFG spectra at different spots of the drop-casted Co_3Fe_2 sample under Ar purging conditions.

5. Single-Crystal X-ray Structure

The single crystal x-ray diffraction studies were carried out on a Bruker Kappa Photon III CPAD diffractometer equipped with Mo K α radiation ($\lambda = 0.71073 \text{ \AA}$). A 0.247 x 0.136 x 0.118 mm piece of a black block was mounted on a Cryoloop with Paratone 24EX oil. Data were collected in a nitrogen gas stream at 100(2) K using ϕ and ω scans. Crystal-to-detector distance was 60 mm using variable exposure time (1 s - 10 s) depending on θ with a scan width of 1.0° . Data collection was 99.9% complete to 25.00° in θ (0.83 \AA). A total of 126125 reflections were collected covering the indices, $-22 \leq h \leq 22$, $-30 \leq k \leq 29$, $-29 \leq l \leq 28$. 21231 reflections were found to be symmetry independent, with a R_{int} of 0.0647. Indexing and unit cell refinement indicated a primitive, monoclinic lattice. The space group was found to be P21/c. The data were integrated using the Bruker SAINT software program and scaled using the SADABS software program. Solution by dual-space method (SHELXT) produced a complete phasing model for refinement.

All nonhydrogen atoms were refined anisotropically by full-matrix least-squares (SHELXL-2014). All hydrogen atoms were placed using a riding model. Their positions were constrained relative to their parent atom using the appropriate HFIX command in SHELXL-2014. Due to unmodelable solvent disorder, OLEX2 solvent mask was used to remove the electron density from the lattice due to the disordered solvent contribution. Solvent appeared to be acetonitrile. One large void was found with approximately 549 electrons, which equates to approximately 24 acetonitrile in the solvent void. The structure is shown below in Figure S13. Crystallographic data are summarized in Tables S3-S6.

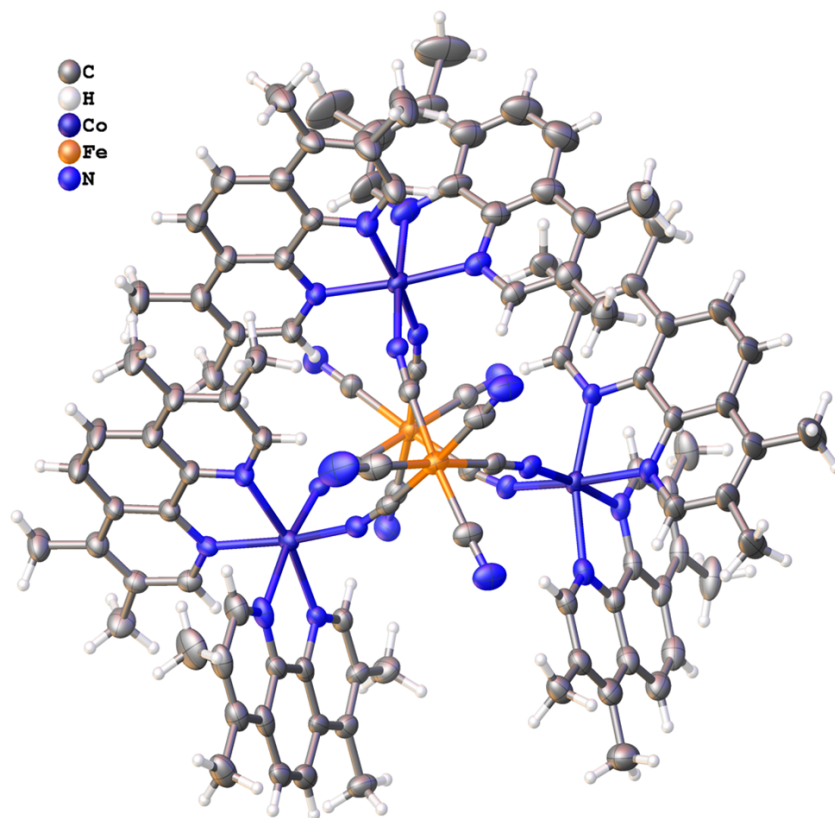


Figure S13: Co_3Fe_2 single x-ray crystal structure.

Table S3: Crystal data and structure refinement for Co_3Fe_2 .

Empirical formula	C120 H114 Co3 Fe2 N30	
Molecular formula	C108 H96 Co3 Fe2 N24, 6[C2H3N]	
Formula weight	2264.90	
Temperature	100.0 K	
Wavelength	0.71073 Å	
Crystal system	Monoclinic	
Space group	P 1 21/c 1	
Unit cell dimensions	a = 18.9918(10) Å b = 24.9372(12) Å c = 24.5780(11) Å	$\alpha = 90^\circ$ $\beta = 97.449(2)^\circ$ $\gamma = 90^\circ$
Volume	11542.0(10) Å ³	
Z	4	
Density (calculated)	1.303 Mg/m ³	
Absorption coefficient	0.729 mm ⁻¹	
F(000)	4708	
Crystal size	0.247 x 0.136 x 0.118 mm ³	
Crystal color, habit	black block	
Theta range for data collection	1.860 to 25.451°	
Index ranges	-22 ≤ h ≤ 22, -30 ≤ k ≤ 29, -29 ≤ l ≤ 28	
Reflections collected	126125	
Independent reflections	21231 [R(int) = 0.0647, R(sigma) = 0.0425]	
Completeness to theta = 25.000°	99.9 %	
Absorption correction	Semi-empirical from equivalents	
Max. and min. transmission	0.0439 and 0.0238	
Refinement method	Full-matrix least-squares on F ²	
Data / restraints / parameters	21231 / 0 / 1258	
Goodness-of-fit on F ²	1.018	
Final R indices [I>2sigma(I)]	R1 = 0.0649, wR2 = 0.1711	
R indices (all data)	R1 = 0.0910, wR2 = 0.1930	
Extinction coefficient	n/a	
Largest diff. peak and hole	1.143 and -0.323 e.Å ⁻³	

Table S4: Atomic coordinates ($\times 10^4$) and equivalent isotropic displacement parameters ($\text{Å}^2 \times 10^3$). U(eq) is defined as one third of the trace of the orthogonalized U^{ij} tensor.

Atom	x	y	z	U(eq)
Co(1)	1446(1)	4535(1)	3364(1)	44(1)
N(1)	658(2)	4816(1)	2773(1)	47(1)
N(2)	1056(2)	3820(1)	3000(2)	53(1)

N(3)	710(2)	4467(1)	3900(2)	55(1)
N(4)	2003(2)	4073(2)	3968(2)	57(1)
C(1)	480(2)	5321(2)	2660(2)	51(1)
C(2)	-139(3)	5471(2)	2326(2)	64(1)
C(3)	-595(3)	5082(2)	2095(2)	76(2)
C(4)	-404(3)	4537(2)	2198(2)	74(2)
C(5)	230(2)	4426(2)	2535(2)	53(1)
C(6)	448(2)	3886(2)	2652(2)	58(1)
C(7)	47(3)	3453(2)	2416(2)	80(2)
C(8)	314(4)	2926(2)	2526(3)	97(2)
C(9)	934(3)	2869(2)	2870(3)	85(2)
C(10)	1288(3)	3323(2)	3098(2)	70(1)
C(11)	-811(3)	4083(2)	1973(3)	103(2)
C(12)	-592(4)	3574(2)	2074(3)	102(2)
C(13)	-283(3)	6060(2)	2236(2)	80(2)
C(14)	-1300(4)	5224(2)	1756(3)	119(3)
C(15)	-103(4)	2444(2)	2296(4)	151(4)
C(16)	1269(4)	2322(2)	3010(3)	114(3)
C(17)	61(3)	4680(2)	3862(2)	66(1)
C(18)	-402(3)	4624(2)	4245(2)	73(1)
C(19)	-174(3)	4345(2)	4726(2)	73(2)
C(20)	512(3)	4107(2)	4786(2)	69(1)
C(21)	928(2)	4183(2)	4353(2)	59(1)
C(22)	1629(3)	3945(2)	4382(2)	59(1)
C(23)	1895(3)	3609(2)	4816(2)	70(1)
C(24)	2584(3)	3376(2)	4809(2)	76(2)
C(25)	2956(3)	3495(2)	4373(2)	66(1)

C(26)	2650(2)	3854(2)	3968(2)	61(1)
C(27)	812(3)	3777(2)	5233(2)	81(2)
C(28)	1458(3)	3536(2)	5253(2)	80(2)
C(29)	-1127(3)	4867(2)	4141(3)	93(2)
C(30)	-647(3)	4277(3)	5168(3)	99(2)
C(31)	2914(4)	3001(3)	5261(3)	102(2)
C(32)	3677(3)	3263(2)	4306(2)	76(1)
Co(1')	4384(1)	6292(1)	3841(1)	47(1)
N(1')	4695(2)	6626(2)	3115(1)	53(1)
N(2')	4854(2)	7043(1)	4120(1)	46(1)
N(3')	5399(2)	5949(2)	4132(2)	64(1)
N(4')	4269(2)	6044(1)	4658(1)	52(1)
C(1')	4598(2)	6428(2)	2615(2)	57(1)
C(2')	4860(3)	6651(2)	2158(2)	64(1)
C(3')	5256(3)	7115(2)	2235(2)	71(1)
C(4')	5349(3)	7356(2)	2767(2)	68(1)
C(5')	5058(2)	7091(2)	3188(2)	54(1)
C(6')	5135(2)	7329(2)	3733(2)	52(1)
C(7')	5473(2)	7825(2)	3836(2)	59(1)
C(8')	5509(3)	8044(2)	4370(2)	62(1)
C(9')	5232(2)	7749(2)	4762(2)	57(1)
C(10')	4919(2)	7255(2)	4616(2)	53(1)
C(11')	5698(3)	7852(2)	2888(2)	88(2)
C(12')	5750(3)	8078(2)	3392(2)	78(2)
C(13')	4702(3)	6387(2)	1612(2)	74(2)
C(14')	5587(4)	7370(3)	1770(2)	103(2)
C(15')	5855(4)	8576(2)	4517(2)	91(2)

C(16')	5257(3)	7951(2)	5345(2)	83(2)
C(17')	5952(3)	5905(2)	3852(3)	81(2)
C(18')	6614(2)	5658(2)	4093(3)	72(1)
C(19')	6663(3)	5456(2)	4612(2)	76(1)
C(20')	6093(2)	5496(2)	4912(2)	66(1)
C(21')	5467(2)	5754(2)	4650(2)	58(1)
C(22')	4867(2)	5811(2)	4938(2)	55(1)
C(23')	4895(3)	5632(2)	5487(2)	61(1)
C(24')	4306(3)	5688(2)	5761(2)	63(1)
C(25')	3707(3)	5933(2)	5489(2)	64(1)
C(26')	3719(2)	6099(2)	4940(2)	55(1)
C(27')	6087(3)	5322(2)	5458(2)	67(1)
C(28')	5542(3)	5385(2)	5729(2)	68(1)
C(29')	7191(3)	5637(3)	3711(3)	116(2)
C(30')	7348(3)	5184(2)	4863(3)	91(2)
C(31')	4346(3)	5486(2)	6344(2)	81(2)
C(32')	3050(3)	6025(2)	5746(2)	82(2)
Co(1")	2075(1)	6327(1)	1683(1)	50(1)
N(1")	1398(2)	5736(2)	1412(2)	64(1)
N(2")	1237(3)	6784(2)	1399(2)	82(1)
N(3")	2400(2)	6474(2)	940(2)	61(1)
N(4")	2734(2)	6957(1)	1893(1)	53(1)
C(1")	1488(3)	5207(2)	1458(2)	62(1)
C(2")	982(3)	4833(2)	1242(2)	73(1)
C(3")	348(3)	5015(3)	949(2)	90(2)
C(4")	237(4)	5585(3)	915(2)	92(2)
C(5")	764(3)	5918(2)	1153(2)	75(1)

C(6")	692(4)	6500(2)	1152(2)	83(2)
C(7")	75(5)	6735(3)	897(3)	110(2)
C(8")	17(5)	7314(3)	923(3)	124(3)
C(9")	597(6)	7591(3)	1175(4)	133(3)
C(10")	1175(5)	7317(2)	1408(3)	110(2)
C(11")	-396(4)	5837(3)	638(3)	126(3)
C(12")	-458(5)	6388(3)	641(3)	128(3)
C(13")	1154(3)	4246(2)	1317(3)	89(2)
C(14")	-190(4)	4621(3)	682(3)	121(3)
C(15")	-688(6)	7573(4)	645(4)	194(6)
C(16")	586(7)	8202(3)	1174(4)	182(5)
C(17")	2214(3)	6227(3)	465(2)	82(2)
C(18")	2429(3)	6400(3)	-37(2)	90(2)
C(19")	2872(3)	6835(3)	-39(2)	79(2)
C(20")	3089(3)	7096(2)	470(2)	66(1)
C(21")	2830(2)	6900(2)	943(2)	57(1)
C(22")	3028(2)	7157(2)	1460(2)	55(1)
C(23")	3497(3)	7596(2)	1517(2)	63(1)
C(24")	3656(3)	7839(2)	2042(2)	66(1)
C(25")	3355(3)	7622(2)	2473(2)	62(1)
C(26")	2905(3)	7183(2)	2378(2)	60(1)
C(27")	3550(3)	7545(2)	533(2)	74(1)
C(28")	3756(3)	7775(2)	1028(2)	75(1)
C(29")	2155(4)	6086(4)	-554(3)	129(3)
C(30")	3134(3)	7025(3)	-551(2)	100(2)
C(31")	4116(3)	8334(2)	2117(2)	85(2)
C(32")	3471(3)	7857(2)	3046(2)	73(1)

Fe(1)	3609(1)	4840(1)	2462(1)	57(1)
N(1F)	2217(2)	4571(1)	2902(1)	52(1)
N(2F)	2853(2)	5818(1)	1893(1)	49(1)
N(3F)	4073(2)	5600(2)	3436(1)	51(1)
N(4F)	5075(3)	5084(3)	2101(3)	129(2)
N(5F)	3142(3)	4189(2)	1413(2)	90(2)
N(6F)	4142(3)	3801(2)	3067(2)	80(1)
C(1F)	2728(3)	4681(2)	2727(2)	50(1)
C(2F)	3170(2)	5458(2)	2098(2)	49(1)
C(3F)	3893(2)	5297(2)	3090(2)	50(1)
C(4F)	4531(3)	4988(3)	2231(2)	84(2)
C(5F)	3323(3)	4424(2)	1806(2)	71(1)
C(6F)	3963(3)	4193(2)	2838(2)	65(1)
Fe(1')	1757(1)	6491(1)	3648(1)	51(1)
N(1F')	1708(2)	5258(2)	3692(1)	51(1)
N(2F')	1761(2)	6321(1)	2413(2)	55(1)
N(3F')	3378(2)	6570(1)	3732(1)	47(1)
N(4F')	1752(2)	7707(2)	3440(2)	81(1)
N(5F')	121(2)	6423(2)	3609(2)	78(1)
N(6F')	1883(2)	6760(2)	4888(2)	76(1)
C(1F')	1760(2)	5715(2)	3716(2)	48(1)
C(2F')	1731(2)	6379(2)	2873(2)	50(1)
C(3F')	2769(2)	6531(2)	3698(2)	46(1)
C(4F')	1739(2)	7255(2)	3523(2)	60(1)
C(5F')	728(3)	6457(2)	3616(2)	62(1)
C(6F')	1842(2)	6647(2)	4424(2)	61(1)

Table S5: Bond lengths [\AA] and angles [$^\circ$] for Co_3Fe_2 .

Co(1)-N(1)	2.069(3)
Co(1)-N(2)	2.087(3)
Co(1)-N(3)	2.049(4)
Co(1)-N(4)	2.060(4)
Co(1)-N(1F)	1.968(4)
Co(1)-N(1F')	2.011(4)
N(1)-C(1)	1.322(5)
N(1)-C(5)	1.352(5)
N(2)-C(6)	1.354(5)
N(2)-C(10)	1.327(6)
N(3)-C(17)	1.333(6)
N(3)-C(21)	1.341(6)
N(4)-C(22)	1.351(6)
N(4)-C(26)	1.345(6)
C(1)-H(1)	0.95
C(1)-C(2)	1.395(6)
C(2)-C(3)	1.373(7)
C(2)-C(13)	1.505(6)
C(3)-C(4)	1.419(7)
C(3)-C(14)	1.524(7)
C(4)-C(5)	1.398(6)
C(4)-C(11)	1.440(7)
C(5)-C(6)	1.428(6)
C(6)-C(7)	1.403(6)
C(7)-C(8)	1.422(7)
C(7)-C(12)	1.416(7)

C(8)-C(9)	1.365(7)
C(8)-C(15)	1.508(7)
C(9)-C(10)	1.396(7)
C(9)-C(16)	1.525(7)
C(10)-H(10)	0.95
C(11)-H(11)	0.95
C(11)-C(12)	1.349(7)
C(12)-H(12)	0.95
C(13)-H(13A)	0.98
C(13)-H(13B)	0.98
C(13)-H(13C)	0.98
C(14)-H(14A)	0.98
C(14)-H(14B)	0.98
C(14)-H(14C)	0.98
C(15)-H(15A)	0.98
C(15)-H(15B)	0.98
C(15)-H(15C)	0.98
C(16)-H(16A)	0.98
C(16)-H(16B)	0.98
C(16)-H(16C)	0.98
C(17)-H(17)	0.95
C(17)-C(18)	1.376(7)
C(18)-C(19)	1.390(8)
C(18)-C(29)	1.496(8)
C(19)-C(20)	1.421(8)
C(19)-C(30)	1.508(7)
C(20)-C(21)	1.415(6)

C(20)-C(27)	1.431(8)
C(21)-C(22)	1.451(7)
C(22)-C(23)	1.398(7)
C(23)-C(24)	1.434(8)
C(23)-C(28)	1.452(7)
C(24)-C(25)	1.390(7)
C(24)-C(31)	1.524(8)
C(25)-C(26)	1.407(7)
C(25)-C(32)	1.515(7)
C(26)-H(26)	0.95
C(27)-H(27)	0.95
C(27)-C(28)	1.361(8)
C(28)-H(28)	0.95
C(29)-H(29A)	0.98
C(29)-H(29B)	0.98
C(29)-H(29C)	0.98
C(30)-H(30A)	0.98
C(30)-H(30B)	0.98
C(30)-H(30C)	0.98
C(31)-H(31A)	0.98
C(31)-H(31B)	0.98
C(31)-H(31C)	0.98
C(32)-H(32A)	0.98
C(32)-H(32B)	0.98
C(32)-H(32C)	0.98
Co(1')-N(1')	2.122(3)
Co(1')-N(2')	2.149(3)

Co(1')-N(3')	2.145(4)
Co(1')-N(4')	2.140(4)
Co(1')-N(3F)	2.040(4)
Co(1')-N(3F')	2.018(4)
N(1')-C(1')	1.315(5)
N(1')-C(5')	1.348(5)
N(2')-C(6')	1.352(5)
N(2')-C(10')	1.320(5)
N(3')-C(17')	1.333(6)
N(3')-C(21')	1.352(6)
N(4')-C(22')	1.377(5)
N(4')-C(26')	1.331(6)
C(1')-H(1')	0.95
C(1')-C(2')	1.402(6)
C(2')-C(3')	1.379(7)
C(2')-C(13')	1.490(6)
C(3')-C(4')	1.428(6)
C(3')-C(14')	1.514(6)
C(4')-C(5')	1.401(6)
C(4')-C(11')	1.417(7)
C(5')-C(6')	1.457(6)
C(6')-C(7')	1.400(6)
C(7')-C(8')	1.414(6)
C(7')-C(12')	1.420(6)
C(8')-C(9')	1.371(6)
C(8')-C(15')	1.503(7)
C(9')-C(10')	1.395(6)

C(9')-C(16')	1.513(6)
C(10')-H(10')	0.95
C(11')-H(11')	0.95
C(11')-C(12')	1.353(7)
C(12')-H(12')	0.95
C(13')-H(13D)	0.98
C(13')-H(13E)	0.98
C(13')-H(13F)	0.98
C(14')-H(14D)	0.98
C(14')-H(14E)	0.98
C(14')-H(14F)	0.98
C(15')-H(15D)	0.98
C(15')-H(15E)	0.98
C(15')-H(15F)	0.98
C(16')-H(16D)	0.98
C(16')-H(16E)	0.98
C(16')-H(16F)	0.98
C(17')-H(17')	0.95
C(17')-C(18')	1.454(8)
C(18')-C(19')	1.365(8)
C(18')-C(29')	1.533(8)
C(19')-C(20')	1.391(7)
C(19')-C(30')	1.524(8)
C(20')-C(21')	1.430(7)
C(20')-C(27')	1.413(7)
C(21')-C(22')	1.425(7)
C(22')-C(23')	1.416(6)

C(23')-C(24')	1.388(7)
C(23')-C(28')	1.433(7)
C(24')-C(25')	1.384(7)
C(24')-C(31')	1.512(7)
C(25')-C(26')	1.415(6)
C(25')-C(32')	1.488(7)
C(26')-H(26')	0.95
C(27')-H(27')	0.95
C(27')-C(28')	1.310(7)
C(28')-H(28')	0.95
C(29')-H(29D)	0.98
C(29')-H(29E)	0.98
C(29')-H(29F)	0.98
C(30')-H(30D)	0.98
C(30')-H(30E)	0.98
C(30')-H(30F)	0.98
C(31')-H(31D)	0.98
C(31')-H(31E)	0.98
C(31')-H(31F)	0.98
C(32')-H(32D)	0.98
C(32')-H(32E)	0.98
C(32')-H(32F)	0.98
Co(1")-N(1")	2.011(4)
Co(1")-N(2")	2.007(5)
Co(1")-N(3")	2.038(4)
Co(1")-N(4")	2.033(4)
Co(1")-N(2F)	1.967(4)

Co(1")-N(2F')	1.962(4)
N(1")-C(1")	1.336(6)
N(1")-C(5")	1.364(7)
N(2")-C(6")	1.333(8)
N(2")-C(10")	1.336(7)
N(3")-C(17")	1.325(6)
N(3")-C(21")	1.340(6)
N(4")-C(22")	1.358(5)
N(4")-C(26")	1.318(5)
C(1")-H(1")	0.95
C(1")-C(2")	1.395(7)
C(2")-C(3")	1.396(8)
C(2")-C(13")	1.506(7)
C(3")-C(4")	1.436(9)
C(3")-C(14")	1.506(9)
C(4")-C(5")	1.372(9)
C(4")-C(11")	1.446(9)
C(5")-C(6")	1.457(8)
C(6")-C(7")	1.386(9)
C(7")-C(8")	1.450(10)
C(7")-C(12")	1.416(11)
C(8")-C(9")	1.377(12)
C(8")-C(15")	1.563(11)
C(9")-C(10")	1.355(11)
C(9")-C(16")	1.523(10)
C(10")-H(10")	0.95
C(11")-H(11")	0.95

C(11")-C(12")	1.379(10)
C(12")-H(12")	0.95
C(13")-H(13G)	0.98
C(13")-H(13H)	0.98
C(13")-H(13I)	0.98
C(14")-H(14G)	0.98
C(14")-H(14H)	0.98
C(14")-H(14I)	0.98
C(15")-H(15G)	0.98
C(15")-H(15H)	0.98
C(15")-H(15I)	0.98
C(16")-H(16G)	0.98
C(16")-H(16H)	0.98
C(16")-H(16I)	0.98
C(17")-H(17")	0.95
C(17")-C(18")	1.415(8)
C(18")-C(19")	1.376(8)
C(18")-C(29")	1.525(8)
C(19")-C(20")	1.424(7)
C(19")-C(30")	1.488(7)
C(20")-C(21")	1.406(6)
C(20")-C(27")	1.418(7)
C(21")-C(22")	1.430(6)
C(22")-C(23")	1.408(6)
C(23")-C(24")	1.421(7)
C(23")-C(28")	1.429(7)
C(24")-C(25")	1.378(6)

C(24")-C(31")	1.510(7)
C(25")-C(26")	1.391(6)
C(25")-C(32")	1.516(6)
C(26")-H(26")	0.95
C(27")-H(27")	0.95
C(27")-C(28")	1.357(7)
C(28")-H(28")	0.95
C(29")-H(29G)	0.98
C(29")-H(29H)	0.98
C(29")-H(29I)	0.98
C(30")-H(30G)	0.98
C(30")-H(30H)	0.98
C(30")-H(30I)	0.98
C(31")-H(31G)	0.98
C(31")-H(31H)	0.98
C(31")-H(31I)	0.98
C(32")-H(32G)	0.98
C(32")-H(32H)	0.98
C(32")-H(32I)	0.98
Fe(1)-C(1F)	1.915(5)
Fe(1)-C(2F)	1.917(4)
Fe(1)-C(3F)	1.938(5)
Fe(1)-C(4F)	1.945(6)
Fe(1)-C(5F)	1.934(5)
Fe(1)-C(6F)	1.937(5)
N(1F)-C(1F)	1.144(6)
N(2F)-C(2F)	1.159(5)

N(3F)-C(3F)	1.157(5)
N(4F)-C(4F)	1.145(8)
N(5F)-C(5F)	1.144(6)
N(6F)-C(6F)	1.155(6)
Fe(1')-C(1F')	1.942(4)
Fe(1')-C(2F')	1.919(5)
Fe(1')-C(3F')	1.912(4)
Fe(1')-C(4F')	1.929(5)
Fe(1')-C(5F')	1.948(5)
Fe(1')-C(6F')	1.934(5)
N(1F')-C(1F')	1.147(5)
N(2F')-C(2F')	1.147(5)
N(3F')-C(3F')	1.152(5)
N(4F')-C(4F')	1.147(6)
N(5F')-C(5F')	1.154(6)
N(6F')-C(6F')	1.165(6)

Table S6: Hydrogen coordinates ($\times 10^4$) and isotropic displacement parameters ($\text{\AA}^2 \times 10^3$).

	x	y	z	U(eq)
H(1)	790	5595	2814	61
H(10)	1719	3273	3335	84
H(11)	-1248	4145	1746	124
H(12)	-876	3288	1912	122
H(13A)	-677	6168	2433	121
H(13B)	-410	6129	1843	121
H(13C)	143	6265	2373	121
H(14A)	-1352	5019	1413	178

H(14B)	-1309	5609	1673	178
H(14C)	-1691	5136	1964	178
H(15A)	-559	2562	2100	227
H(15B)	-188	2204	2596	227
H(15C)	166	2253	2042	227
H(16A)	958	2112	3217	171
H(16B)	1731	2370	3232	171
H(16C)	1333	2132	2670	171
H(17)	-95	4887	3545	79
H(26)	2914	3947	3679	73
H(27)	547	3724	5531	97
H(28)	1625	3316	5558	96
H(29A)	-1486	4582	4122	139
H(29B)	-1176	5063	3793	139
H(29C)	-1195	5114	4440	139
H(30A)	-990	3989	5065	149
H(30B)	-901	4613	5213	149
H(30C)	-357	4184	5515	149
H(31A)	2664	3039	5583	154
H(31B)	3416	3093	5361	154
H(31C)	2875	2630	5130	154
H(32A)	3824	3392	3961	114
H(32B)	3648	2871	4298	114
H(32C)	4024	3377	4614	114
H(1')	4329	6108	2559	69
H(10')	4738	7055	4896	64
H(11')	5902	8032	2606	105

H(12')	5978	8416	3451	94
H(13D)	4441	6636	1351	110
H(13E)	4412	6066	1646	110
H(13F)	5147	6284	1479	110
H(14D)	5254	7629	1579	155
H(14E)	5695	7091	1513	155
H(14F)	6026	7554	1918	155
H(15D)	5507	8820	4645	136
H(15E)	6030	8730	4193	136
H(15F)	6253	8525	4809	136
H(16D)	5749	8032	5494	124
H(16E)	5070	7675	5571	124
H(16F)	4968	8277	5348	124
H(17')	5914	6038	3488	97
H(26')	3302	6262	4757	66
H(27')	6499	5150	5638	80
H(28')	5577	5264	6098	82
H(29D)	7637	5777	3904	173
H(29E)	7045	5855	3384	173
H(29F)	7260	5265	3601	173
H(30D)	7266	4799	4899	137
H(30E)	7503	5337	5226	137
H(30F)	7718	5242	4625	137
H(31D)	4520	5115	6363	122
H(31E)	3873	5499	6462	122
H(31F)	4672	5712	6586	122
H(32D)	3149	6280	6049	124

H(32E)	2889	5684	5887	124
H(32F)	2678	6170	5472	124
H(1")	1922	5077	1649	75
H(10")	1562	7518	1589	132
H(11")	-768	5624	454	151
H(12")	-882	6543	462	153
H(13G)	754	4061	1451	134
H(13H)	1580	4204	1585	134
H(13I)	1239	4090	965	134
H(14G)	10	4429	390	182
H(14H)	-618	4814	525	182
H(14I)	-312	4365	957	182
H(15G)	-683	7586	246	291
H(15H)	-730	7938	785	291
H(15I)	-1093	7357	727	291
H(16G)	952	8337	1459	273
H(16H)	118	8328	1248	273
H(16I)	680	8334	815	273
H(17")	1920	5919	462	99
H(26")	2708	7036	2681	72
H(27")	3721	7690	217	89
H(28")	4082	8065	1050	90
H(29G)	1896	6329	-823	194
H(29H)	1836	5801	-461	194
H(29I)	2557	5927	-709	194
H(30G)	3631	6917	-548	151
H(30H)	3098	7416	-573	151

H(30I)	2846	6865	-870	151
H(31G)	4422	8351	1825	127
H(31H)	4411	8319	2474	127
H(31I)	3814	8654	2100	127
H(32G)	3215	8198	3051	110
H(32H)	3980	7919	3154	110
H(32I)	3295	7606	3304	110

6. DFT-Optimized Structures

Coordinates (in Å) are provided for structures optimized at the B(35)LYP/def2-SV(P) level: the $S = 3/2$ state, corresponding to the low-spin configuration $(\text{Co}^{2+})(\text{Co}^{3+})_2(\text{Fe}^{2+})_2$, and the $S = 9/2$ state with the configuration $(\text{Co}^{2+})_3(\text{Fe}^{3+})_2$.

A. $S = 3/2$ state

Co	3.669561	0.847376	0.115931
N	3.917066	2.844589	0.931450
N	4.629373	1.974897	-1.502443
C	3.431745	3.252114	2.088551
H	2.958049	2.497396	2.720666
C	3.474975	4.597947	2.520305
C	4.073988	5.535123	1.680872
C	4.581690	5.104691	0.421464
C	5.130850	5.993925	-0.564985
H	5.248680	7.047248	-0.319026
C	5.461159	5.556757	-1.814512
H	5.829479	6.270588	-2.548234
C	5.284326	4.185108	-2.203964
C	5.410822	3.721428	-3.544446
C	5.052526	2.406810	-3.830656
C	4.687968	1.571148	-2.751599
H	4.384941	0.542938	-2.951991
C	4.853007	3.271635	-1.221887
C	4.476048	3.738694	0.092318
C	2.853078	4.939378	3.851174

H	3.606028	5.348198	4.546106
H	2.071880	5.707583	3.729956
H	2.390602	4.051318	4.315980
C	4.156297	6.991247	2.054038
H	5.184111	7.369085	1.938651
H	3.514127	7.597783	1.392805
H	3.837627	7.162649	3.088477
C	5.846350	4.671419	-4.627919
H	6.100343	4.138768	-5.551982
H	5.042408	5.390077	-4.861310
H	6.726040	5.253490	-4.314214
C	4.989838	1.833168	-5.222665
H	4.547011	2.554225	-5.925246
H	5.996678	1.576688	-5.597342
H	4.358375	0.929983	-5.229478
N	5.577313	0.190262	1.059005
N	4.142625	-1.141627	-0.791990
C	6.231422	0.843498	1.991074
H	5.838545	1.825186	2.257186
C	7.375197	0.347708	2.652844
C	7.840892	-0.912725	2.295451
C	7.133337	-1.638039	1.298179
C	7.497857	-2.959832	0.877308
H	8.385203	-3.426610	1.299162
C	6.747165	-3.646522	-0.030154
H	7.049303	-4.650635	-0.319640
C	5.564270	-3.082043	-0.614635

C	4.718173	-3.793771	-1.515198
C	3.644646	-3.120424	-2.082062
C	3.410558	-1.782133	-1.677871
H	2.580708	-1.237369	-2.120721
C	5.216657	-1.763347	-0.265072
C	5.997960	-1.040130	0.709651
C	8.024779	1.193218	3.717782
H	9.077971	1.409872	3.476932
H	7.495870	2.150749	3.827571
H	8.007703	0.686588	4.695965
C	9.048456	-1.530742	2.947879
H	9.509130	-0.859162	3.681364
H	8.774041	-2.464441	3.464915
H	9.808818	-1.790568	2.194134
C	5.008999	-5.243185	-1.801298
H	5.928962	-5.355618	-2.399492
H	5.160547	-5.792543	-0.859915
H	4.185835	-5.726282	-2.338868
C	2.697144	-3.697320	-3.098846
H	1.790302	-4.086645	-2.607823
H	2.373239	-2.896380	-3.782460
H	3.161893	-4.499392	-3.688251
Co	-0.936949	-3.265092	-0.133079
N	0.866250	-3.783375	0.491634
N	-0.925375	-5.099065	-0.909192
C	1.743047	-3.064650	1.169714
H	1.498793	-2.028389	1.368144

C	2.962831	-3.602806	1.645835
C	3.271314	-4.927312	1.364246
C	2.379931	-5.671783	0.540910
C	2.613480	-7.008096	0.068512
H	3.543710	-7.504497	0.330872
C	1.718652	-7.668235	-0.719854
H	1.959812	-8.670682	-1.062165
C	0.469889	-7.069921	-1.101376
C	-0.521188	-7.684447	-1.913142
C	-1.682120	-6.966754	-2.201230
C	-1.833680	-5.676395	-1.668801
H	-2.731913	-5.102817	-1.885398
C	0.216612	-5.762129	-0.632435
C	1.177538	-5.057719	0.156955
C	3.846256	-2.750900	2.504207
H	4.907430	-2.955428	2.309287
H	3.634524	-1.686909	2.344487
H	3.610674	-2.960649	3.559732
C	4.512569	-5.533400	1.954369
H	5.412837	-5.083608	1.509747
H	4.549753	-5.311502	3.031572
H	4.563207	-6.621291	1.828372
C	-0.364363	-9.065156	-2.486123
H	0.523235	-9.589638	-2.117523
H	-1.247961	-9.678323	-2.250253
H	-0.301382	-9.012973	-3.585757
C	-2.768473	-7.534750	-3.072560

H	-3.178071	-8.465790	-2.647470
H	-3.592714	-6.817077	-3.189272
H	-2.383550	-7.780455	-4.075455
N	-1.820793	-3.856139	1.544134
N	-2.797117	-2.960555	-0.743233
C	-1.264695	-4.033746	2.733383
H	-0.179462	-4.055220	2.786618
C	-2.010867	-4.076862	3.925717
C	-3.401502	-3.990946	3.857636
C	-4.006758	-3.882523	2.578714
C	-5.421435	-3.874913	2.327362
H	-6.102719	-4.087151	3.146829
C	-5.930573	-3.627805	1.088085
H	-7.005161	-3.667630	0.932721
C	-5.079023	-3.272207	-0.011600
C	-5.542632	-2.865544	-1.289664
C	-4.608857	-2.465963	-2.243888
C	-3.234576	-2.509891	-1.908386
H	-2.490576	-2.180011	-2.631367
C	-3.692198	-3.327571	0.201583
C	-3.160741	-3.729681	1.465786
C	-1.303876	-4.108729	5.246544
H	-0.223325	-4.228359	5.118196
H	-1.460248	-3.133420	5.736431
H	-1.712201	-4.899003	5.897814
C	-4.183995	-3.876281	5.128425
H	-3.916373	-2.894836	5.558969

H	-5.269652	-3.910434	4.979576
H	-3.898828	-4.656458	5.849322
C	-7.017572	-2.894703	-1.579704
H	-7.586027	-2.418147	-0.770128
H	-7.259908	-2.383333	-2.516592
H	-7.368466	-3.938355	-1.653560
C	-4.999172	-2.018279	-3.626841
H	-4.137425	-1.603770	-4.173716
H	-5.424151	-2.859682	-4.200587
H	-5.767517	-1.233916	-3.576513
Co	-2.701632	2.512794	0.180459
N	-4.185659	1.335221	0.722686
N	-3.713742	2.641562	-1.518441
C	-3.256835	3.069635	-2.685507
H	-2.328265	3.635208	-2.688945
C	-3.848582	2.712169	-3.910743
C	-5.004426	1.929550	-3.900707
C	-5.554049	1.554699	-2.646427
C	-6.782959	0.834089	-2.451459
H	-7.430573	0.655835	-3.306267
C	-7.168680	0.380749	-1.226018
H	-8.117068	-0.140346	-1.136029
C	-6.316410	0.508634	-0.074457
C	-6.558782	-0.057433	1.205242
C	-5.556156	0.016642	2.173562
C	-4.360996	0.707095	1.875175
H	-3.552595	0.755834	2.605755

C	-5.123563	1.235298	-0.244164
C	-4.810518	1.859183	-1.493532
C	-3.175911	3.081440	-5.197977
H	-3.885722	3.556912	-5.895009
H	-2.310849	3.729573	-5.022872
H	-2.797343	2.154285	-5.659765
C	-5.532830	1.409010	-5.201653
H	-6.469699	0.847981	-5.100295
H	-5.682753	2.222241	-5.927970
H	-4.754167	0.735475	-5.604935
C	-7.861438	-0.719544	1.558234
H	-8.292354	-0.236744	2.449921
H	-8.603244	-0.672892	0.753108
H	-7.698718	-1.772647	1.826708
C	-5.734249	-0.587275	3.537714
H	-4.774273	-0.630498	4.078329
H	-6.459963	0.001968	4.126446
H	-6.138163	-1.606405	3.453597
N	-3.609833	4.101126	0.969949
N	-1.346385	3.847122	-0.320008
C	-4.743190	4.155766	1.640165
H	-5.292079	3.224578	1.757384
C	-5.248463	5.339608	2.201127
C	-4.522945	6.521665	2.051421
C	-3.295241	6.476074	1.339426
C	-2.419168	7.592612	1.121568
H	-2.692954	8.572157	1.503523

C	-1.238924	7.454782	0.453110
H	-0.610428	8.331808	0.325115
C	-0.797902	6.193407	-0.074802
C	0.429813	5.971862	-0.765418
C	0.724582	4.682960	-1.188845
C	-0.191158	3.640157	-0.917327
H	0.057080	2.624693	-1.188221
C	-1.651601	5.093111	0.111740
C	-2.885573	5.230320	0.816288
C	-6.546266	5.302655	2.960705
H	-6.404334	5.635475	4.001540
H	-7.293874	5.973684	2.506697
H	-6.963107	4.285610	2.981294
C	-5.062334	7.782002	2.667637
H	-4.479525	8.673910	2.414995
H	-6.102314	7.947968	2.346169
H	-5.082623	7.684900	3.765693
C	1.947931	4.357845	-1.987047
H	2.787270	5.011192	-1.727716
H	2.232863	3.309470	-1.843572
H	1.701983	4.469100	-3.055739
C	1.412245	7.076255	-1.048380
H	1.638063	7.110063	-2.125006
H	1.057475	8.066397	-0.740621
H	2.365409	6.871703	-0.534666
Fe	-0.115532	0.046514	3.203460
N	-0.880067	-1.615850	0.742042

C	-0.687788	-0.971793	1.695246
N	-1.739273	2.229488	1.781732
C	-1.045585	1.504926	2.387921
N	1.278006	2.116581	5.111928
C	0.688695	1.274784	4.563811
N	1.229876	-2.646202	4.125298
C	0.738911	-1.610853	3.904164
N	-2.750190	-0.883992	4.663436
C	-1.764754	-0.464520	4.199842
N	2.569606	0.277357	1.714857
C	1.543672	0.289038	2.270187
Fe	-0.120953	0.161231	-3.087987
N	-0.202359	-2.588925	-1.747227
C	-0.109026	-1.591886	-2.357972
N	-1.856998	1.107419	-0.737403
C	-1.323034	0.649607	-1.666234
N	-0.276945	3.208856	-3.874820
C	-0.199739	2.061006	-3.682909
N	2.438868	-0.534601	-4.770221
C	1.399941	-0.266906	-4.312050
N	-2.596053	-0.374171	-4.962317
C	-1.623856	-0.237087	-4.332526
N	2.048385	1.015224	-1.084566
C	1.245806	0.683534	-1.855876

A. $S = 9/2$ state

Co	3.743588	0.161117	-0.041151
----	----------	----------	-----------

N	4.358528	2.080840	0.746616
N	4.880528	1.056941	-1.674744
C	3.997866	2.586018	1.910062
H	3.391227	1.951237	2.557055
C	4.341676	3.886424	2.339442
C	5.121529	4.670674	1.492372
C	5.508708	4.136767	0.230161
C	6.256463	4.870947	-0.753220
H	6.611919	5.869094	-0.507517
C	6.491823	4.362253	-1.996717
H	7.025406	4.965277	-2.728122
C	6.015413	3.062591	-2.382428
C	6.076019	2.559191	-3.712914
C	5.457848	1.342935	-3.992253
C	4.898160	0.621832	-2.915268
H	4.410707	-0.334539	-3.109155
C	5.368177	2.282316	-1.404942
C	5.092266	2.831719	-0.099257
C	3.829551	4.352093	3.679000
H	4.659283	4.648227	4.341450
H	3.175246	5.231303	3.559919
H	3.249608	3.561310	4.181919
C	5.534251	6.069154	1.863278
H	6.629017	6.181690	1.811515
H	5.100329	6.796612	1.159112
H	5.208292	6.335866	2.875226
C	6.736305	3.376318	-4.790142

H	6.867990	2.800363	-5.713533
H	6.129644	4.266422	-5.028031
H	7.724975	3.732623	-4.462450
C	5.327653	0.768671	-5.379083
H	5.036814	1.546869	-6.099630
H	6.281214	0.332822	-5.724864
H	4.546369	-0.006566	-5.398971
N	5.470931	-0.836103	0.918083
N	3.743026	-1.903927	-0.855141
C	6.289764	-0.292831	1.789411
H	6.170428	0.777359	1.960050
C	7.276876	-1.005639	2.500993
C	7.394658	-2.371304	2.263783
C	6.505835	-2.974947	1.332903
C	6.507695	-4.379152	1.039751
H	7.238484	-5.020860	1.526259
C	5.606391	-4.924288	0.175833
H	5.638264	-5.993132	-0.019043
C	4.623299	-4.124349	-0.497015
C	3.664923	-4.655349	-1.407965
C	2.823319	-3.771781	-2.070487
C	2.903728	-2.399851	-1.740201
H	2.244008	-1.698471	-2.242156
C	4.614049	-2.737013	-0.248389
C	5.552671	-2.160455	0.684906
C	8.142825	-0.263718	3.486037
H	9.209141	-0.326904	3.215134

H	7.862727	0.798783	3.522842
H	8.035734	-0.674652	4.502268
C	8.413209	-3.218467	2.977661
H	9.094373	-2.616751	3.590752
H	7.914078	-3.946770	3.637866
H	9.016106	-3.793493	2.258028
C	3.587799	-6.136826	-1.660950
H	4.336676	-6.448171	-2.410022
H	3.773892	-6.708621	-0.743236
H	2.596729	-6.423217	-2.031880
C	1.834506	-4.196867	-3.121914
H	0.900011	-4.556220	-2.661241
H	1.577895	-3.341896	-3.762401
H	2.248615	-4.998295	-3.750804
Co	-1.532481	-3.057704	-0.242648
N	0.225684	-4.073949	0.561315
N	-1.761609	-5.122260	-0.938364
C	1.186168	-3.537636	1.281944
H	1.135504	-2.463817	1.436954
C	2.249554	-4.276222	1.854980
C	2.282321	-5.646334	1.635255
C	1.269643	-6.230400	0.821828
C	1.234797	-7.625461	0.489027
H	2.015718	-8.277294	0.873889
C	0.258949	-8.152274	-0.301092
H	0.287189	-9.213499	-0.532077
C	-0.801416	-7.338821	-0.829352

C	-1.851759	-7.827767	-1.655350
C	-2.817988	-6.929969	-2.106003
C	-2.719632	-5.584840	-1.708571
H	-3.463193	-4.859112	-2.041284
C	-0.800918	-5.959952	-0.503264
C	0.253612	-5.400393	0.314671
C	3.251401	-3.545287	2.701826
H	4.273210	-3.894037	2.505241
H	3.196244	-2.466294	2.513528
H	3.009055	-3.693512	3.765062
C	3.339349	-6.530416	2.239411
H	4.049851	-5.961213	2.846636
H	2.875361	-7.296280	2.881469
H	3.905865	-7.062355	1.458601
C	-1.957243	-9.268407	-2.078297
H	-1.255970	-9.930405	-1.559567
H	-2.976040	-9.643801	-1.897931
H	-1.775573	-9.359327	-3.162409
C	-3.949837	-7.363306	-2.996684
H	-4.574607	-8.127752	-2.505694
H	-4.591787	-6.509850	-3.257327
H	-3.573261	-7.808624	-3.931829
N	-2.763430	-3.425365	1.540252
N	-3.535418	-2.523205	-0.895421
C	-2.291919	-3.622406	2.756493
H	-1.233191	-3.866538	2.846065
C	-3.054566	-3.446217	3.923679

C	-4.398512	-3.100637	3.789449
C	-4.933248	-2.947719	2.481925
C	-6.313681	-2.671649	2.192702
H	-7.038328	-2.685684	3.002922
C	-6.744631	-2.406937	0.929830
H	-7.801838	-2.226754	0.760718
C	-5.829061	-2.311329	-0.172935
C	-6.199297	-1.879434	-1.476056
C	-5.201584	-1.723478	-2.435670
C	-3.877598	-2.055914	-2.080176
H	-3.073529	-1.926644	-2.805633
C	-4.476084	-2.637817	0.065215
C	-4.043927	-3.045132	1.387527
C	-2.403810	-3.561393	5.270213
H	-1.354007	-3.862604	5.176541
H	-2.418672	-2.573348	5.757407
H	-2.945753	-4.273234	5.915544
C	-5.181337	-2.802042	5.034356
H	-4.736547	-1.902182	5.493098
H	-6.245924	-2.614266	4.854304
H	-5.088132	-3.621661	5.762824
C	-7.642179	-1.627605	-1.824144
H	-8.196891	-1.175207	-0.993625
H	-7.734182	-0.962704	-2.690040
H	-8.140946	-2.580580	-2.073843
C	-5.477827	-1.220512	-3.827301
H	-4.545882	-1.084776	-4.392487

H	-6.141472	-1.909797	-4.376113
H	-5.979031	-0.241180	-3.789120
Co	-2.132477	3.106556	0.168201
N	-4.004393	2.196270	0.850518
N	-3.362110	3.383618	-1.477894
C	-2.895772	3.729992	-2.665064
H	-1.910642	4.194518	-2.686043
C	-3.548147	3.431440	-3.872881
C	-4.792264	2.802230	-3.818098
C	-5.343828	2.502406	-2.543783
C	-6.648408	1.936271	-2.327733
H	-7.322791	1.824760	-3.172984
C	-7.073966	1.555281	-1.091757
H	-8.078107	1.157324	-0.976603
C	-6.203727	1.611350	0.050020
C	-6.532267	1.096951	1.334632
C	-5.548151	1.085855	2.320746
C	-4.282351	1.633887	2.007967
H	-3.479191	1.603593	2.747540
C	-4.929343	2.186832	-0.126215
C	-4.541818	2.738349	-1.405411
C	-2.870296	3.710527	-5.182221
H	-2.668708	2.753710	-5.689882
H	-3.511416	4.320593	-5.840914
H	-1.904019	4.206538	-5.032740
C	-5.429684	2.366328	-5.104804
H	-6.438373	1.955485	-4.979912

H	-5.476876	3.197319	-5.825244
H	-4.782950	1.585600	-5.542774
C	-7.928956	0.610967	1.614818
H	-7.976887	0.015130	2.532787
H	-8.612734	1.469833	1.731077
H	-8.316929	-0.002947	0.792691
C	-5.775027	0.529574	3.700989
H	-4.829910	0.477841	4.259368
H	-6.497813	1.145498	4.263045
H	-6.184173	-0.489136	3.645240
N	-2.505357	4.921513	1.069531
N	-0.414268	4.304440	-0.454240
C	-3.560685	5.200283	1.804584
H	-4.332931	4.433820	1.851169
C	-3.718900	6.397811	2.522232
C	-2.703268	7.349545	2.468642
C	-1.551626	7.063766	1.685382
C	-0.416810	7.935702	1.554626
H	-0.415777	8.891869	2.070704
C	0.670443	7.595505	0.806471
H	1.497839	8.297678	0.742162
C	0.745686	6.349834	0.095081
C	1.856541	5.936841	-0.704483
C	1.775929	4.712289	-1.356757
C	0.612443	3.928582	-1.172964
H	0.544572	2.959268	-1.650943
C	-0.364658	5.487186	0.184697

C	-1.507502	5.829736	0.994159
C	-4.964897	6.611826	3.337637
H	-4.722415	6.780549	4.399490
H	-5.523399	7.496840	2.990246
H	-5.628701	5.738076	3.272348
C	-2.867034	8.622501	3.253614
H	-2.081250	9.359573	3.058326
H	-3.837818	9.088412	3.023939
H	-2.869900	8.403335	4.334405
C	2.798449	4.159492	-2.307393
H	3.770071	4.661336	-2.244390
H	2.934641	3.085349	-2.122061
H	2.404553	4.242250	-3.333573
C	3.068035	6.819513	-0.860091
H	2.983377	7.442714	-1.766862
H	3.204235	7.491724	-0.003569
H	3.979927	6.218561	-0.958873
Fe	0.016807	0.079369	3.349785
N	-1.112696	-1.344419	0.818703
C	-0.825425	-0.796240	1.795626
N	-1.082023	2.504780	1.742339
C	-0.567205	1.719280	2.418714
N	1.847685	1.767560	5.226450
C	1.099916	1.079366	4.664744
N	0.697000	-2.807027	4.355412
C	0.467586	-1.701207	4.084756
N	-2.719779	-0.138062	4.861399

C	-1.683341	-0.024165	4.350067
N	2.582887	-0.205665	1.606314
C	1.659395	-0.023735	2.282712
Fe	-0.103813	0.314765	-3.355002
N	-0.665049	-2.445656	-2.032711
C	-0.409675	-1.479934	-2.622168
N	-1.582125	1.561558	-0.921148
C	-1.166110	1.056423	-1.873146
N	0.277100	3.280933	-4.277556
C	0.137177	2.160644	-4.006781
N	2.234142	-0.927018	-5.014574
C	1.282248	-0.448406	-4.550743
N	-2.673792	0.137692	-5.141164
C	-1.680729	0.160240	-4.539712
N	2.150146	0.648987	-1.233000
C	1.321490	0.540819	-2.031573

References

- (1) Berlinguette, C. P.; Dragulescu-Andrasi, A.; Sieber, A.; Galán-Mascarós, J. R.; Güdel, H.-U.; Achim, C.; Dunbar, K. R. A charge-transfer-induced spin transition in the discrete cyanide-bridged complex $\{[\text{Co}(\text{tmphen})_2]_3[\text{Fe}(\text{CN})_6]_2\}$. *Journal of the American Chemical Society* **2004**, *126*, 6222–6223.
- (2) Klyuev, Y. A. Vibrational spectra of crystalline potassium ferri-and ferrocyanide. *Journal of Applied Spectroscopy* **1965**, *3*, 30–34.
- (3) Berlinguette, C. P.; Dragulescu-Andrasi, A.; Sieber, A.; Güdel, H.-U.; Achim, C.; Dunbar, K. R. A charge-transfer-induced spin transition in a discrete complex: the role of extrinsic factors in stabilizing three electronic isomeric forms of a cyanide-bridged Co/Fe cluster. *Journal of the American Chemical Society* **2005**, *127*, 6766–6779.
- (4) Moulder, J. F.; Stickle, W. F.; Sobol, P. E.; Bomben, K. D.; Chastain, J. *Handbook of X-ray Photoemission Spectroscopy*; Perkin-Elmer Corporation, Minnesota, 1992.
- (5) Shimamoto, N.; Ohkoshi, S.-i.; Sato, O.; Hashimoto, K. Control of charge-transfer-induced spin transition temperature on cobalt-iron Prussian blue analogues. *Inorganic chemistry* **2002**, *41*, 678–684.
- (6) Grosvenor, A.; Kobe, B.; Biesinger, M.; McIntyre, N. Investigation of multiplet splitting of Fe 2p XPS spectra and bonding in iron compounds. *Surface and Interface Analysis* **2004**, *36*, 1564–1574.
- (7) Lykhach, Y.; Piccinin, S.; Skala, T.; Bertram, M.; Tsud, N.; Brummel, O.; Farnesi Camellone, M.; Beranova, K.; Neitzel, A.; Fabris, S. et al. Quantitative analysis of the oxidation state of cobalt oxides by resonant photoemission spectroscopy. *The Journal of Physical Chemistry Letters* **2019**, *10*, 6129–6136.

- (8) Biesinger, M. C.; Payne, B. P.; Grosvenor, A. P.; Lau, L. W.; Gerson, A. R.; Smart, R. S. C. Resolving surface chemical states in XPS analysis of first row transition metals, oxides and hydroxides: Cr, Mn, Fe, Co and Ni. *Applied Surface Science* **2011**, *257*, 2717–2730.
- (9) Cabrera-German, D.; Gomez-Sosa, G.; Herrera-Gomez, A. Accurate peak fitting and subsequent quantitative composition analysis of the spectrum of Co 2p obtained with Al K α radiation: I: Cobalt spinel. *Surface and Interface Analysis* **2016**, *48*, 252–256.